Induction of angiotensin converting enzyme after miR-143/145 deletion is critical for impaired smooth muscle contractility.

Dahan, Diana; Ekman, Mari; Larsson Callerfelt, Anna-Karin; Turczynska, Karolina; Boettger, Thomas; Braun, Thomas; Swärd, Karl; Albinsson, Sebastian

Published in:
American Journal of Physiology: Cell Physiology

DOI:
10.1152/ajpcell.00250.2014

2014

Document Version:
Peer reviewed version (aka post-print)

Induction of angiotensin converting enzyme after miR-143/145 deletion is critical for impaired smooth muscle contractility*

[1a]Diana Dahan, [2a]Mari Ekman, [1]Anna-Karin Larsson-Callerfelt, [1]Karolina Turczyńska, [3]Thomas Boettger, [3]Thomas Braun, [1b]Karl Swärd, and [1b]Sebastian Albinsson

From the [1]Department of Experimental Medical Science, Lund University, Sweden, [2]Department of Biology, Lund University, Sweden, [3]Max Planck Institute for Heart and Lung Research, Bad Nauheim, Germany.

[*]Running title: *Differential effects of miR-143/145 deletion in smooth muscle*

[a]These authors share first authorship
[b]These authors share senior authorship

To whom correspondence should be addressed: Sebastian Albinsson, Department of Experimental Medical Science, Lund University, BMC D12, 221 84 Lund, Sweden, Tel.: +46-46-2220678; Fax: +46-46-2224546; E-mail: sebastian.albinsson@med.lu.se

Keywords: angiotensin II, contractile protein, microRNA (miRNA), smooth muscle, vascular biology, detrusor, airway, urinary bladder, miR-145, myocardin

---

ABSTRACT

MicroRNAs have emerged as regulators of smooth muscle cell phenotype with a role in smooth muscle-related disease. Studies have shown that miR-143 and miR-145 are the most highly expressed microRNAs in smooth muscle cells, controlling differentiation and function. The effect of miR-143/145 knockout has been established in the vasculature but not in smooth muscle from other organs.

Using knockout mice we found that maximal contraction induced by either depolarization or phosphatase inhibition was reduced in vascular and airway smooth muscle but maintained in the urinary bladder. Furthermore, a reduction of media thickness and reduced expression of differentiation markers was seen in the aorta but not in the bladder. Supporting the view that phenotype switching depends on a tissue-specific target of miR-143/145, we found induction of angiotensin converting enzyme in the aorta but not in the bladder where angiotensin converting enzyme was expressed at a low level. Chronic treatment with angiotensin type-1 receptor antagonist restored contractility in miR-143/145-deficient aorta while leaving bladder contractility unaffected. This shows that tissue-specific targets are critical for the effects of miR-143/145 on smooth muscle differentiation and that angiotensin converting enzyme is one such target.

-

Smooth muscle cells play an important role in the formation and function of the cardiovascular, digestive, respiratory, and urinary systems. The ability of smooth muscle cells to contract and relax is crucial for the regulation of blood pressure, for peristaltic movements in the gut and for micturition. Furthermore, smooth muscle cells can modulate their phenotype to a less contractile, more proliferative and migratory state in response to local environmental cues (30). This phenotype, often referred to as "synthetic", is associated with decreased expression of contractile markers and

increased synthesis of extracellular matrix proteins.

Recently, microRNAs (miRNAs) have emerged as regulators of smooth muscle cell phenotype with important roles in disease progression (5, 6). MiRNAs are short non-coding RNAs (18-25 nucleotides long) with complementarity to sequences in target mRNAs (7). Biogenesis of most miRNAs requires the endonuclease dicer, which cleaves a pre-miRNA to generate a mature miRNA that in turn regulates mRNA stability and protein translation. Since hundreds of miRNAs are expressed in a cell, most signaling pathways are controlled by this class of RNAs. MiRNAs show promise as therapeutic targets as they can be manipulated using mimics and inhibitors (36).

Several studies have shown that miR-143 and miR-145 are among the most highly expressed miRNAs in differentiated smooth muscle (8, 10, 11, 32, 39). They are encoded by a bicistronic miRNA cluster regulated by the transcription factor serum response factor (SRF) and its co-factors myocardin and myocardin related transcription factors (MRTFs) (11, 24, 39). The expression of both miR-143 and miR-145 is dramatically down-regulated in phenotypically modulated smooth muscle cell following vascular injury (10, 11). Furthermore, while both miR-143 and miR-145 are thought to be involved in the regulation of smooth muscle proliferation and migration (15, 39) it is primarily miR-145 that promotes contractile differentiation of vascular smooth muscle (5). Several mechanisms have been proposed for miR-145-dependent regulation of vascular smooth muscle differentiation, including direct or indirect up-regulation of myocardin (10, 11), regulation of actin polymerization (3, 39), and control of calcium signaling (33, 34). Furthermore, miR-145 regulates the expression of angiotensin converting enzyme (ACE) and this was demonstrated to play a significant role for the effects of miR-143/145 knockout (KO) in vascular smooth muscle (8).

Using smooth muscle-specific and tamoxifen-inducible KO of dicer, we previously found that loss of miRNAs impairs smooth muscle cell differentiation in the aorta, leading to reduced contractility and blood pressure (4). Using the same mouse model we also demonstrated impaired depolarization-induced contraction in the urinary bladder (32). Expression of smooth muscle differentiation markers was however hardly affected in the bladder, contrasting with our findings in the aorta. Possible explanations for this discrepancy include the presence of miRNAs that repress differentiation in bladder smooth muscle cells. Alternatively, miRNAs with an established role in smooth muscle differentiation, such as miR-143/145, may act on targets that are unique for the vasculature. Here we addressed this possibility by comparing contractility and differentiation in aorta, airways and urinary bladder from miR-143/145 KO mice. While contractility and differentiation were diminished in aorta, loss of miR-143/145 had no effect on bladder contractility and increased rather than decreased expression of differentiation markers. These effects correlated with induction of ACE, which was expressed at a low level and not induced in the bladder of KO mice. Finally, blockade of angiotensin receptors rescued contractility in the aorta but was without effect in the bladder, arguing that ACE is a key target for miR-143/145-dependent phenotype switching in smooth muscle cells.

EXPERIMENTAL PROCEDURES

Animals

All animal experiments were approved by the Malmö/Lund animal ethics committee (M167-09, M287-12). The miR-143/145 KO mice were generated at the Max-Planck-Institute for Heart and Lung Research as described previously (8) and bred in-house.

β-Galactosidase staining

To generate KO mice the miR-143/145 locus was targeted with a vector containing the LacZ reporter (8). β-Galactosidase activity was used as a reporter of miR-143/145 expression. Micro-dissected organs from male and female heterozygous mice were fixed in 4% paraformaldehyde in phosphate-buffered saline (pH 7.0) for 10 min at 4 °C. Organs were then incubated with continuous shaking in X-gal staining solution (150 mM NaCl, 2 mM MgCl2, 5 mM potassium ferricyanide, 5 mM potassium ferrocyanide, 40 mM citric acid, 12 mM sodium

phosphate, pH 6.0) containing 1 mg/ml X-gal (Sigma, St. Louis, MO) at 37 °C overnight. Photographs were acquired with an Infinity 1 camera mounted on an Olympus (SZ61) microscope.

Hemodynamic measurements
Systemic blood pressure was recorded using tail cuffs (CODA Non-invasive Blood Pressure System, Kent Scientific Corporation) as described previously (4). Animals were trained for 5 consecutive days prior to blood pressure recordings. The blood pressure of each animal was then recorded 3 times.

Isometric force measurements
Aortic and tracheal rings and bladder strips (1.5 - 2 mm length) were mounted in a Mulvany myograph (610M, Danish Myo Technology) and bathed in HEPES-buffered Kreb's solution (in mM : 135.5 NaCl, 5.9 KCl, 2.5 $CaCl_2$, 1.2 $MgCl_2$, 11.6 HEPES; pH 7.4) at 37°C. During an equilibration period of 30 minutes the preparations were stretched to a stable passive tension of 5mN (aorta), 1mN (trachea) and 8mN (bladder). After this period, each experiment was started by exposing the preparations twice to 60mM KCl-containing HEPES solution. Following each contraction, preparations were relaxed in normal HEPES buffer. Cumulative concentration-responses curves for cirazoline and angiotensin II (aorta) or carbachol (bladder, trachea) were generated. At the end of each experiment, 1µM CalyculinA was applied following relaxation in calcium-free HEPES buffer.

Precision-cut lung slices (PCLS)
To investigate if there were any differences in contractility in more distal airways we used PCLS as previously described (20). Lungs were filled with pre-warmed agarose solution (0.75%) via the trachea and subsequently chilled with ice. The lung lobes were separated and cut into 250 ± 20 µm thick slices with a Krumdieck tissue slicer (Alabama Research and Development, Munford, AL). Slices were incubated in minimal essential medium (MEM) supplemented with vitamins, glutamine, sodium pyruvate, non-essential amino acids and 1 % penicillin/streptomycin. For measurements, slices with comparable airway area were selected, covered with 1 ml of medium and fixed with a nylon thread attached to a platinum wire to avoid movements. Images were recorded using a Nikon Eclipse microscope and a Nikon DS-2Mv (Nikon, Tokyo, Japan) digital camera. Cumulative doses of carbachol were maintained for 7 min. Images were analyzed using NIS Elements AR (Nikon, Tokyo, Japan). Airway area before addition of any drug was defined as 100%. Airway contractions were expressed as a percentage of the initial airway area.

Histology
Aortae were fixed in 4% paraformaldehyde for 30 minutes, washed in PBS containing 10% sucrose, followed by embedding in OCT (Tissue Tek, Sakura). Frozen sections (10µm) were cut in a cryostat. The urinary bladders were freed from adhering adipose tissue and emptied and a small cut at the bladder base was made to allow for entry of fixative (4% formaldehyde in PBS for 24h at 4°C). Samples were then washed in 70% ethanol, dehydrated through increasing ethanol and xylene, and embedded in paraffin wax. 3 µm equatorial sections from the middle part of the urinary bladders were cut using a microtome (Microm HM340E, Fisher Scientific). Before staining, sections were deparafinized and boiled in 0.01 M citrate buffer. Tissue sections from both aorta and urinary bladder were stained with hematoxylin and eosin (Sigma-Aldrich) following the manufacturer's instructions and the thickness of the smooth muscle cell layer was determined using a computerized image-analysis system (Olympus CellSens dimension software).

Quantitative real-time PCR (qRT-PCR)
Total RNA was isolated using the miRNeasy mini kit (Qiagen) according to the manufacturer's instructions. mRNA was detected using the QuantiFast SYBR Green RT-PCR Kit (Qiagen). For miRNA measurements, 500ng of template RNA was reverse transcribed to cDNA using miScript II RT Kit (Qiagen) according to the manufacturer's instructions. RT-qPCR was performed using a StepOnePlus qPCR machine (Applied Biosystems).

Western blot

Aorta and bladder were excised, cleaned and quickly frozen in liquid nitrogen. The samples were homogenized in sodium dodecyl sulphate (SDS) sample buffer (60 mM Tris-HCl, pH 6.8, 2% SDS, 10% glycerol) as previously described (32). The amount of protein was determined using Biorad´s DC protein assay. Equal amounts (20µg) of protein was loaded in the wells of Bio-Rad TGX 4-15% or Any KD Criterion gels, then transferred using wet transfer over-night. Proteins were detected using the following commercially available primary antibodies: HSP-90 (610418, BD Transduction Laboratories), ACE (ab39172, Abcam), Rho-kinase (ACC-003 #4035 (C8F7) Cell signaling), phospho-LIM-kinase (#3841, Cell signaling), LIM-kinase (#3842, Cell signaling). After washing, membranes were immersed in HRP-conjugated secondary antibodies (#7074, 7076, Cell signaling). Membranes were incubated with Super Signal West Femto chemiluminescence substrate (Pierce), according to the manufacturer's instructions. Immunoblots were acquired using the Odyssey Fc Imager (LI- COR Biosciences). Band densities were quantified using Image Studio software (LI- COR Biosciences).

F/G actin assay

F to G-actin ratio was determined by using the G-actin/F-actin in vivo assay kit (cytoskeleton). Briefly, the G-actin and F- actin pools were separated by ultracentrifugation at 100,000g during 1h at 37°C and the supernatant was diluted in 5X SDS sample buffer. The pellet was resuspended in F- actin depolymerizing buffer and kept on ice during 1h and then diluted with 5X SDS sample buffer. The same amount of supernatant and pellet fraction (10µL) was loaded on Bio-Rad TGX 4-15% Criterion gels. Proteins were transferred to nitrocellulose membrane using Trans Turbo Blot device (Bio-Rad) for 10min at 2.5 A. The membrane was then incubated with rabbit smooth muscle alpha-actin antibody (provided with the kit, Cat. #AAN01). Anti-rabbit HRP-conjugated secondary antibody (#7076, Cell Signaling) was used. Images were acquired using the Odyssey Fc Imager (LI-COR Biosciences).

Organ culture

Aortic rings and bladder strips were prepared and organ cultured with 100 µg/ml of losartan (Tocris) at 37°C and 5% CO2/air in a humidified incubator. Strips were maintained in DMEM/Ham's F12 medium (Biochrom, FG4815) supplemented with 50U/ml Penicillin and 50ug/ml Streptomycin (Biochrom, A2213). Strips were harvested for isometric force experiments after 5 days of culture.

Statistics

Values are presented as mean ± S.E.M. n-values refer to the number of mice. Mann-Whitney or Student's unpaired t-test (one or two-tailed as appropriate) or ANOVA was used to test for significance using GraphPad Prism 5 (GraphPad Software Inc.). Concentration-response curves were compared using repeated measures ANOVA. Differences were considered significant at $p<0.05$.

RESULTS

Differential effect of miR-143/145 deletion on contractility in the aorta, airway and urinary bladder

As previously demonstrated (8), we found that expression of the miR-143/145 cluster was enriched in smooth muscle cells (figure 1A) and that deletion of this cluster results in reduced mean systemic blood pressure (WT:153.5±8.9 mmHg vs KO:119.5±7.8 mmHg). Since the aim of this study was to compare the effect of miR-143/145 KO in different smooth muscle containing tissues we first evaluated the baseline expression of these miRNAs in wild type (WT) aorta, airway and bladder. The expression level was comparable in aorta and bladder but significantly lower in airways (figure 1B). We then assessed agonist-induced contractile function using the α_1-adrenergic receptor agonist cirazoline in the aorta and the muscarinic receptor agonist carbachol in the bladder and airways. The contractile response to cirazoline (figure 1C) was significantly reduced in aorta from miR-143/145 KO mice. The response to carbachol was unchanged in the bladder (figure 1D) as was the cholinergic component of neurogenic activation by electrical field stimulation (data not shown). We also assessed the response to carbachol in

bronchioles using precision-cut lung slices (figure 1E), but, similar to bladder, no significant effect was seen. Interestingly, depolarization-induced contraction (60mM KCl) was reduced in aorta and trachea but unaffected in the urinary bladder (figure 1F-H). To test if the reduced ability of the different KO preparations to generate force was due to a change in the contractile machinery of the smooth muscle cells we used the phosphatase inhibitor calyculin A. Contraction induced by calyculin A was decreased in aorta and trachea but was unchanged in the bladder from miR-143/145 KO mice (figure 1I-K). In summary, this indicates a defect in the contractility in the aorta and in the airways but not in the urinary bladder. We focused henceforth on the aorta and urinary bladder because of the contrasting effects of miR-143/145 deletion on contractility in these tissues.

Smooth muscle differentiation markers are reduced in the aorta but not in the urinary bladder of miR-143/145 KO mice

Smooth muscle differentiation markers were next analyzed by qRT-PCR. We noted down-regulation of mRNAs for myosin heavy chain (*Myh11*), desmin (*Des*) and L-type Ca^{2+} channels (*Cacna1c*) in the aorta of miR-143/145 KO mice (figure 2A). Surprisingly these differentiation markers were unaffected or changed in the opposite direction in the urinary bladder (figure 2B). Expression of smooth muscle markers depends on myocardin and serum response factor (SRF)-driven transcription. In keeping with the effect on contractile smooth muscle cell markers, we observed a reduction of myocardin and SRF expression in the aorta but up-regulation of myocardin and unchanged SRF expression in the urinary bladder (compare figure 2A and 2B). No significant change in krüppel-like factor 4 (KLF4) and KLF5 mRNAs was observed in either aorta or bladder. Together, these findings favored the idea that some tissue-specific miRNA target upstream of myocardin might be responsible for altered smooth muscle marker expression in miR-143/145-deficient smooth muscle.

Using conventional histology we observed a reduction of the thickness of the smooth muscle layer in miR-143/145 KO aorta (figure 2C, 2D). In the bladder, no significant difference of the smooth muscle layer thickness was seen (figure 2C, 2E).

The differential effect of miR-143/145 KO is not due to reduced Rho activation and actin polymerization or altered KLF4/5 expression

The miR-143/145 cluster has previously been suggested to modulate cytoskeletal dynamics by targeting proteins in the Rho/Rho-kinase pathway (39), which is involved in the regulation of both gene expression and contractile function in smooth muscle (18, 28). Rho-activation promotes the expression of contractile genes in smooth muscle by stimulation of actin polymerization and subsequent nuclear translocation of the myocardin related transcription factor (MRTF), a co-factor for serum response factor (SRF) (28). In order to determine if the Rho/Rho-kinase pathway was differentially affected by miR-143/145 deletion in aorta vs. bladder we analyzed protein expression of ROCK-1 and phosphorylation levels of LIMK which is downstream of Rho-kinase. The expression level of ROCK1 was significantly higher in aorta compared to bladder, and was higher in KO bladder than WT bladder (figure 3A). ROCK1 also tended to be higher in KO versus WT aorta, but this difference did not reach statistical significance. The phosphorylation level of LIMK was increased in KO aorta but unchanged in bladder (figure 3B). To directly address if this was associated with a differential effect on actin polymerization in aorta and bladder we measured the F to G-actin ratio. While the F to G-actin ratio appeared to be higher in the bladder compared to the aorta, no difference was seen between WT and KO in either tissue (figure 3C). Thus, our findings do not strongly support a primary role of altered actin polymerization in the differential effect of miR-143/145 deletion on contractile differentiation in aorta and bladder.

It has been suggested that the KLF4 can repress the expression of contractile markers in smooth muscle by down-regulating myocardin expression and by preventing SRF binding to smooth muscle gene promoters (23). Both KLF4 and KLF 5 have been confirmed as targets for miR-145 in vascular smooth muscle (10, 11). However, we did not find a significant difference in KLF4 expression and only a slight increase KLF 5 in KO bladder.

MiR-143/145 deletion increases angiotensin converting enzyme (ACE) expression in aorta but not in bladder

An additional mechanism by which the miR-143/145 cluster has been proposed to drive smooth muscle contractile differentiation is via repression of angiotensin converting enzyme (ACE). To address if this mechanism might underlie the difference between aorta and bladder we first performed qRT-PCR for ACE. A significant up-regulation of ACE mRNA was seen in aorta but not in the bladder of KO mice (Figure 4A). Furthermore, the total ACE expression was much higher in the aorta compared to the bladder. The differential effect on ACE in aorta and bladder was seen also when protein expression was analyzed by western blotting (figure 4B). Although the protein expression level of ACE in bladder was low, we were able to detect a band at the correct molecular weight after longer exposure (data not shown).

We next tested if the contractile response to angiotensin II was altered in miR-143/145 KO smooth muscle. As shown in figure 4C, the maximal contractile response to angiotensin II was significantly reduced in aorta from miR-143/145 KO mice. No response to angiotensin II was seen in the bladder. This difference is illustrated by the force responses in aorta and bladder at 0.1 μM angiotensin II (figure 4D). These findings suggested that lack of impact of miR143/145 on bladder contractility could be due to lack of ACE induction and lack of responsiveness to angiotensin II. To test this hypothesis, we incubated aortic rings and bladder strips with the angiotensin receptor blocker losartan for five days in organ culture and measured contractile function in a myograph. Losartan was not present in the solution during the isometric force recordings. In KO aorta, losartan treatment increased the contractile response to cirazoline (figure 5A) and to calyculin A (figure 5C). In WT aorta, losartan slightly reduced cirazoline-induced contraction (Figure 5A). In the bladder, losartan treatment was without effect on both carbachol (figure 5B) and calyculin A (figure 5D) responses irrespective of genotype. However, following organ culture, an increased contractile response to carbachol was observed in the miR-143/145 bladder.

Differential effects of miR-143/145 deletion on mRNA expression of RGS4 and RGS5 and angiotensin receptors.

Increased production of angiotensin II has been previously associated with bi-phasic changes in the expression of RGS4 and RGS5 (Regulators of a G protein Signaling) (38). Furthermore, reduced expression of RGS4/5 mRNA has previously been suggested to be associated with angiotensin II resistance in miR-143/145 KO vascular smooth muscle (8). We therefore predicted that the mRNA levels of RGS4 and RGS5 would be altered in miR-143/145 KO aorta. In keeping with this prediction, we found that both mRNAs were reduced in KO vs. WT aorta but not in KO vs. WT bladder (figure 6A, B). Moreover, basal RGS4 and RGS5 expression was lower in bladder than in aorta.

To examine if reduced angiotensin II responsiveness was associated with altered receptor expression, we finally surveyed receptor mRNA levels. AT_1 receptor mRNA was increased in KO vs. WT aorta whereas no change was seen in KO vs. WT bladder (figure 6C). AT_2 receptor expression was not different KO vs. WT aorta, but its expression was several-fold higher in bladder vs. aorta (figure 6D).

DISCUSSION

Our study addressed the role of miR-143/145 for contractility and contractile differentiation in vascular, airway and bladder smooth muscle. A major finding was that miR-143/145 deletion has varying effects on smooth muscles from different anatomical locations with no or only modest effects on the bladder and major effects on both contractility and differentiation in the aorta. On a general level it is difficult to reconcile these findings with the view that miR-143 and miR-145 influence smooth muscle contractility via hundreds of small effects on targets of relevance for differentiation (8). If this was the case, one would have predicted graded and unidirectional changes in differentiation and contractility in all tissues. This was not seen, and key differentiation

markers, such as smooth muscle myosin (*Myh11*), even changed in opposite directions in aorta and bladder. Therefore, our study favors the view that miR-143 and miR-145 influence contractility and differentiation via a small number of tissue-specific targets.

The pro-contractile effect of miR-143/145 has been attributed in part to up-regulation of myocardin and downregulation of KLF4/5 (10-12, 25). A transcriptional complex consisting of SRF and its co-factors Myocardin, and MRTFs drives gene expression via so called CArG boxes in the promoter regions of smooth muscle differentiation marker genes (27). This effect is counteracted by KLF4-mediated inhibition of SRF binding to CArG containing regions (23). Furthermore, KLF5, which is suppressed by miR-145, negatively regulates myocardin expression in smooth muscle (10). Interestingly, myocardin was upregulated in KO bladder (vs. WT bladder) and down-regulated in KO aorta, supporting a role for myocardin in the differential regulation of contractile smooth muscle marker expression. However, our findings do not support a role for KLF4/5 in this effect, although we cannot completely exclude this possibility. A mechanism upstream of myocardin that depends on a tissue-specific target of miR-143/145 provides a more likely primary explanation.

Previous studies (26) including work by us (1, 2, 41) have shown that actin polymerization is an important stimulus for contractile differentiation in smooth muscle. The mechanism behind this effect involves sequestration of MRTF in the cytoplasm by monomeric G-actin (28). When G-actin is incorporated into filaments (F-actin) MRTF is liberated and translocates to the nucleus where SRF-dependent transcription of contractile and cytoskeletal genes is stimulated (37). Prior work implicated changes in cytoskeletal dynamics as an important factor behind the effects of miR-143/145 on smooth muscle cell fate (5, 39). However, herein we did not find a significant difference in actin polymerization after deletion of miR-143/145 in either aortic or bladder smooth muscle. Our findings therefore do not strongly support altered basal actin polymerization as the reason for the differential impact of miR-143/145 deletion on contractility in aorta and bladder.

ACE was originally found to be upregulated in miR-143/145 KO mice by Boettger et al. (8) using mass spectrometry. Sequences in the 3' UTR of mouse ACE were found to confer sensitivity to miR-145 overexpression in a reporter assay (8), and subsequent work has confirmed regulation of human ACE expression by both miR-143 and miR-145 (19). Our findings agree well with those prior reports and demonstrates robust upregulation of ACE mRNA and protein (>4-fold) in the aorta of KO mice. Compared to the aorta, ACE was expressed at a lower level in the mouse bladder, providing a straightforward explanation for the lack of effect on contractility in miR-143/145 KO bladder. That is, if the target (e.g. ACE) is not expressed at a sufficient level then the miRNAs would be ineffective and their loss would not have an impact on cellular function. The ratio between miRNA and target mRNA is an important determinant for the relative effect of a miRNA (22) and the miR145/ACE ratios do indeed differ considerably in bladder and aorta (compare Figure 1B and 4A). The study of Mukherji et al. (29) demonstrates that an increased mRNA expression saturates the pool of miRNAs leading to dampening of the fold repression. Conversely, when mRNA expression is below to a certain threshold, the absolute effect of miRNA inhibition is irrelevant for protein expression and cellular function.

The cleavage product resulting from ACE activity, angiotensin II, has multiple effects on both contractility and differentiation. Apart from inducing acute contraction, it is well known that short-term treatment with angiotensin II promotes hypertrophy and contractile differentiation of smooth muscle cells in culture (13, 35). So how can increased ACE expression be reconciled with reduced contractile differentiation in the miR-143/145-deficient aorta? To explain this Boettger et al. (8) proposed a model whereby an increase of the local angiotensin II production, not associated with an increased circulating plasma level, induces a state of "angiotensin resistance" (21) with reduced responsiveness not only to angiotensin II but also to other agonists. This

model may be extended to explain reduced differentiation provided that the low level of angiotensin II normally present in the arterial wall provides a drive for differentiation that is lost at higher levels of angiotensin II due to "angiotensin resistance". Here we found that blockade of angiotensin receptors reduced contractility in the WT aorta, consistent with the view that angiotensin II below a certain threshold is pro-contractile and can induce myocardin as well as smooth muscle marker expression (40). In KO aorta on the other hand, where "angiotensin resistance" had been elicited due to the several-fold higher production of angiotensin II, the antagonist improved contractility, presumably because receptor blockade prevented "angiotensin resistance". The "angiotensin resistance" model moreover predicts that miR-143/145 deletion should be without effect on contractility in the absence of ACE induction or in the absence of responsiveness to angiotensin II. Our findings in the bladder confirm this prediction.

Tachyphylaxis ("angiotensin resistance") of AT_1 receptors is a complex process involving internalization, phosphorylation, arrestin binding and uncoupling from downstream signaling pathways (17). Alas, receptor internalization is not readily studied in intact tissue with native, untagged, receptors. Prolonged AT_1 receptor activation does however affect expression of RGS4 and RGS5 mRNAs (38). These mRNAs were therefore used as readouts for angiotensin II signaling. Consistent with our finding that ACE induction is specific for aorta, we show that RGS4 and 5 were repressed in KO aorta but not in KO bladder. However, the importance of this effect for the phenotype shift in miR-143/145 KO aorta is likely to be rather complex and will require further investigation. Available evidence regarding AT_1 receptor mRNA in tachyphylaxis has demonstrated a transient increase followed by sustained repression (31), but the length of these phases could depend on angiotensin II concentration. Here we found that the type 1 receptor was modestly up-regulated in KO aorta. This effect was not seen in bladder, further supporting our view that overall changes in contractility associate with changes in angiotensin II signaling.

Interestingly, contractile function in miR-143/145 KO aorta was partly rescued following organ culture in the presence of the AT_1 receptor antagonist losartan. While our work substantiates an association between altered ACE expression/angiotensin II signaling and loss of contractility in miR-143/145 KO aorta, we cannot associate this with certainty to the AT_1 receptor. In order to maximize the rescue effect in organ culture we used a concentration of losartan that may have affected AT_2 receptors in addition to AT_1 receptors. Furthermore, it is quite possible that other peptides cleaved by ACE (such as bradykinin or angiotensin 1-7) contribute in the KO setting. It is also interesting to note that AT_2 receptor levels were much higher in bladder than in aorta, contrasting with AT_1 receptor levels which were similar. AT_2 receptors are considered to counteract the effects of AT_1 receptors in many regards (9). Elevated AT_2 receptor expression in the bladder may thus impart insensitivity to angiotensin II stimulation and counteract effects of miR-143/145 deletion.

Our prior work using smooth muscle-specific dicer KO mice (32) documented three major phenotypes in the bladder. We reported: 1) increased matrix area between smooth muscle cells, 2) reduced depolarization-induced contraction, and 3) a pronounced impairment of the cholinergic component of neurogenic bladder activation. We have subsequently attributed the increased matrix area in the dicer KO bladder to miR-29 (14) which targets multiple extracellular matrix proteins, but the miRNAs responsible for the reduction of depolarization-induced contraction and impaired neurogenic activation have not been identified. We show here that depolarization-induced contraction and neurogenic activation is maintained in miR-143/145 KO bladders, arguing that miRNAs other than miR-143/145 must be responsible for reduced depolarization-induced contraction and neurogenic activation in dicer KO bladders.

One aim of our study was to also assess the effect of miR-143/145 deletion on airway function. These experiments revealed clear-cut reductions of both depolarization- and phosphatase inhibitor-induced contraction. The airways therefore behave like the aorta in regard to miR-143/145

deletion and ACE is known to be expressed in the airways. This is illustrated by the common adverse effect referred to as "ACE-inhibitor cough"(16) which is due to irritant accumulation of bradykinin in the airways. We did not include airway preparations in our further analyses due to the apparent similarity with the aorta, but these results indicate that miR-143/145 play roles for smooth muscle contractility beyond the vascular system.

In summary, we have shown that tissue-specific targets are decisive for the effects of miR-143/145 on smooth muscle differentiation and that ACE is an important target for miR-143/145-dependent phenotype switching. These findings may have implications for our understanding of phenotypic modulation of smooth muscle cells in disease. Furthermore, our results demonstrate that one miRNA cluster can have contrasting effects in the same cell type from different organs. It remains to be investigated if miR-143/145 and other miRNAs can have varying effects also in different vascular beds. This would have implications for the use of miRNA-targeted therapies in treatment of vascular disease.

REFERENCES

1. **Albinsson S and Hellstrand P.** Integration of signal pathways for stretch-dependent growth and differentiation in vascular smooth muscle. *Am J Physiol Cell Physiol* 293: C772-782, 2007.
2. **Albinsson S, Nordström I, and Hellstrand P.** Stretch of the vascular wall induces smooth muscle differentiation by promoting actin polymerization. *J Biol Chem* 279: 34849-34855, 2004.
3. **Albinsson S and Sessa WC.** Can microRNAs control vascular smooth muscle phenotypic modulation and the response to injury? *Physiol Genomics*, 2010.
4. **Albinsson S, Skoura A, Yu J, Dilorenzo A, Fernandez-Hernando C, Offermanns S, Miano JM, and Sessa WC.** Smooth Muscle miRNAs Are Critical for Post-Natal Regulation of Blood Pressure and Vascular Function. *PLoS One* 6: e18869, 2011.
5. **Albinsson S, Suarez Y, Skoura A, Offermanns S, Miano JM, and Sessa WC.** MicroRNAs are necessary for vascular smooth muscle growth, differentiation, and function. *Arterioscler Thromb Vasc Biol* 30: 1118-1126, 2010.
6. **Albinsson S and Swärd K.** Targeting smooth muscle microRNAs for therapeutic benefit in vascular disease. *Pharmacological research : the official journal of the Italian Pharmacological Society* 75: 28-36, 2013.
7. **Bartel DP.** MicroRNAs: genomics, biogenesis, mechanism, and function. *Cell* 116: 281-297, 2004.
8. **Boettger T, Beetz N, Kostin S, Schneider J, Kruger M, Hein L, and Braun T.** Acquisition of the contractile phenotype by murine arterial smooth muscle cells depends on the Mir143/145 gene cluster. *J Clin Invest* 119: 2634-2647, 2009.
9. **Bosnyak S, Welungoda IK, Hallberg A, Alterman M, Widdop RE, and Jones ES.** Stimulation of angiotensin AT2 receptors by the non-peptide agonist, Compound 21, evokes vasodepressor effects in conscious spontaneously hypertensive rats. *Br J Pharmacol* 159: 709-716, 2010.
10. **Cheng Y, Liu X, Yang J, Lin Y, Xu DZ, Lu Q, Deitch EA, Huo Y, Delphin ES, and Zhang C.** MicroRNA-145, a novel smooth muscle cell phenotypic marker and modulator, controls vascular neointimal lesion formation. *Circ Res* 105: 158-166, 2009.
11. **Cordes KR, Sheehy NT, White MP, Berry EC, Morton SU, Muth AN, Lee TH, Miano JM, Ivey KN, and Srivastava D.** miR-145 and miR-143 regulate smooth muscle cell fate and plasticity. *Nature* 460: 705-710, 2009.
12. **Davis-Dusenbery BN, Chan MC, Reno KE, Weisman AS, Layne MD, Lagna G, and Hata A.** down-regulation of Kruppel-like factor-4 (KLF4) by microRNA-143/145 is critical for modulation of vascular smooth muscle cell

phenotype by transforming growth factor-beta and bone morphogenetic protein 4. *J Biol Chem* 286: 28097-28110, 2011.

13. **di Gioia CR, van de Greef WM, Sperti G, Castoldi G, Todaro N, Ierardi C, Pieruzzi F, and Stella A.** Angiotensin II increases calponin expression in cultured rat vascular smooth muscle cells. *Biochemical and biophysical research communications* 279: 965-969, 2000.

14. **Ekman M, Bhattachariya A, Dahan D, Uvelius B, Albinsson S, and Swärd K.** Mir-29 repression in bladder outlet obstruction contributes to matrix remodeling and altered stiffness. *PLoS One* 8: e82308, 2013.

15. **Elia L, Quintavalle M, Zhang J, Contu R, Cossu L, Latronico MV, Peterson KL, Indolfi C, Catalucci D, Chen J, Courtneidge SA, and Condorelli G.** The knockout of miR-143 and -145 alters smooth muscle cell maintenance and vascular homeostasis in mice: correlates with human disease. *Cell death and differentiation* 16: 1590-1598, 2009.

16. **Fox AJ, Lalloo UG, Belvisi MG, Bernareggi M, Chung KF, and Barnes PJ.** Bradykinin-evoked sensitization of airway sensory nerves: a mechanism for ACE-inhibitor cough. *Nat Med* 2: 814-817, 1996.

17. **Holloway AC, Qian H, Pipolo L, Ziogas J, Miura S, Karnik S, Southwell BR, Lew MJ, and Thomas WG.** Side-chain substitutions within angiotensin II reveal different requirements for signaling, internalization, and phosphorylation of type 1A angiotensin receptors. *Mol Pharmacol* 61: 768-777, 2002.

18. **Kimura K, Ito M, Amano M, Chihara K, Fukata Y, Nakafuku M, Yamamori B, Feng J, Nakano T, Okawa K, Iwamatsu A, and Kaibuchi K.** Regulation of myosin phosphatase by Rho and Rho-associated kinase (Rho-kinase). *Science* 273: 245-248, 1996.

19. **Kohlstedt K, Trouvain C, Boettger T, Shi L, Fisslthaler B, and Fleming I.** AMP-activated protein kinase regulates endothelial cell angiotensin-converting enzyme expression via p53 and the post-transcriptional regulation of microRNA-143/145. *Circulation research* 112: 1150-1158, 2013.

20. **Larsson-Callerfelt AK, Dahlen SE, Kuhl AR, Lex D, Uhlig S, and Martin C.** Modulation of antigen-induced responses by serotonin and prostaglandin E2 via EP1 and EP4 receptors in the peripheral rat lung. *Eur J Pharmacol* 699: 141-149, 2013.

21. **Lassegue B, Alexander RW, Nickenig G, Clark M, Murphy TJ, and Griendling KK.** Angiotensin II down-regulates the vascular smooth muscle AT1 receptor by transcriptional and post-transcriptional mechanisms: evidence for homologous and heterologous regulation. *Molecular pharmacology* 48: 601-609, 1995.

22. **Leung AK and Sharp PA.** MicroRNA functions in stress responses. *Mol Cell* 40: 205-215, 2010.

23. **Liu Y, Sinha S, McDonald OG, Shang Y, Hoofnagle MH, and Owens GK.** Kruppel-like factor 4 abrogates myocardin-induced activation of smooth muscle gene expression. *J Biol Chem* 280: 9719-9727, 2005.

24. **Long X and Miano JM.** Transforming growth factor-beta1 (TGF-beta1) utilizes distinct pathways for the transcriptional activation of microRNA 143/145 in human coronary artery smooth muscle cells. *J Biol Chem* 286: 30119-30129, 2011.

25. **Lovren F, Pan Y, Quan A, Singh KK, Shukla PC, Gupta N, Steer BM, Ingram AJ, Gupta M, Al-Omran M, Teoh H, Marsden PA, and Verma S.** MicroRNA-145 targeted therapy reduces atherosclerosis. *Circulation* 126: S81-90, 2012.

26. **Mack CP, Somlyo AV, Hautmann M, Somlyo AP, and Owens GK.** Smooth muscle differentiation marker gene expression is regulated by RhoA-mediated actin polymerization. *J Biol Chem* 276: 341-347, 2001.

27. **Miano JM.** Dicing up microRNA gene expression profiles in normal and neoplastic smooth muscle cells. *Am J Pathol* 177: 541-543, 2010.

28. **Miralles F, Posern G, Zaromytidou AI, and Treisman R.** Actin dynamics control SRF activity by regulation of its coactivator MAL. *Cell* 113: 329-342, 2003.

29. **Mukherji S, Ebert MS, Zheng GX, Tsang JS, Sharp PA, and van Oudenaarden A.** MicroRNAs can generate thresholds in target gene expression. *Nat Genet* 43: 854-859, 2011.

30. **Owens GK, Kumar MS, and Wamhoff BR.** Molecular regulation of vascular smooth muscle cell differentiation in development and disease. *Physiol Rev* 84: 767-801, 2004.
31. **Richard DE, Laporte SA, Bernier SG, Leduc R, and Guillemette G.** Desensitization of AT1 receptor-mediated cellular responses requires long term receptor down-regulation in bovine adrenal glomerulosa cells. *Endocrinology* 138: 3828-3835, 1997.
32. **Sadegh MK, Ekman M, Rippe C, Uvelius B, Swärd K, and Albinsson S.** Deletion of dicer in smooth muscle affects voiding pattern and reduces detrusor contractility and neuroeffector transmission. *PLoS One* 7: e35882, 2012.
33. **Turczynska KM, Hellstrand P, Swärd K, and Albinsson S.** Regulation of vascular smooth muscle mechanotransduction by microRNAs and L-type calcium channels. *Commun Integr Biol* 6: e22278, 2013.
34. **Turczynska KM, Sadegh MK, Hellstrand P, Swärd K, and Albinsson S.** MicroRNAs are essential for stretch-induced vascular smooth muscle contractile differentiation via microRNA (miR)-145-dependent expression of L-type calcium channels. *J Biol Chem* 287: 19199-19206, 2012.
35. **Turla MB, Thompson MM, Corjay MH, and Owens GK.** Mechanisms of angiotensin II- and arginine vasopressin-induced increases in protein synthesis and content in cultured rat aortic smooth muscle cells. Evidence for selective increases in smooth muscle isoactin expression. *Circulation research* 68: 288-299, 1991.
36. **van Rooij E and Olson EN.** MicroRNAs: powerful new regulators of heart disease and provocative therapeutic targets. *The Journal of clinical investigation* 117: 2369-2376, 2007.
37. **Wang DZ, Li S, Hockemeyer D, Sutherland L, Wang Z, Schratt G, Richardson JA, Nordheim A, and Olson EN.** Potentiation of serum response factor activity by a family of myocardin-related transcription factors. *Proc Natl Acad Sci U S A* 99: 14855-14860, 2002.
38. **Wang X, Adams LD, Pabon LM, Mahoney WM, Jr., Beaudry D, Gunaje J, Geary RL, Deblois D, and Schwartz SM.** RGS5, RGS4, and RGS2 expression and aortic contractibility are dynamically co-regulated during aortic banding-induced hypertrophy. *J Mol Cell Cardiol* 44: 539-550, 2008.
39. **Xin M, Small EM, Sutherland LB, Qi X, McAnally J, Plato CF, Richardson JA, Bassel-Duby R, and Olson EN.** MicroRNAs miR-143 and miR-145 modulate cytoskeletal dynamics and responsiveness of smooth muscle cells to injury. *Genes Dev* 23: 2166-2178, 2009.
40. **Yoshida T, Hoofnagle MH, and Owens GK.** Myocardin and Prx1 contribute to angiotensin II-induced expression of smooth muscle alpha-actin. *Circ Res* 94: 1075-1082, 2004.
41. **Zeidan A, Nordstrom I, Albinsson S, Malmqvist U, Sward K, and Hellstrand P.** Stretch-induced contractile differentiation of vascular smooth muscle: sensitivity to actin polymerization inhibitors. *Am J Physiol Cell Physiol* 284: C1387-1396, 2003.

FOOTNOOTES

*This work was supported by the Swedish Research Council; the Swedish Heart and Lung Foundation, the Crafoord Foundation; the Royal Physiographic Society; the Åke Wiberg Foundation; Olle Engkvist Byggmästare Foundation, the Jeansson Foundation; the Tore Nilson Foundation; the Greta and Johan Kock Foundation; the Magnus Bergvall Foundation, the Zoegas foundation and the Lars Hierta Memorial Foundation. K.M.T. was in part supported by the European Union FP7 Marie Curie Initial Training Network Small Artery Remodeling (SmArt).

[4]The abbreviations used are: MicroRNAs (miRNAs), angiotensin converting enzyme (ACE), Krüppel-like factor-4 and 5 (KLF4/5), Precision-cut lung slices (PCLS)

FIGURE LEGENDS

Figure 1. Differential effect of miR-143/145 deletion on contractility in the aorta and urinary bladder
MiR-143/145 reporter staining demonstrates expression in all smooth muscle cells throughout the body, including the aorta, skeletal muscle arterioles, trachea and bladder (**A**). Quantitative PCR analysis of miR-145 and miR-143 in aortic, airway and bladder smooth muscle (**B**, n=4). MiRNA levels were normalized to WT aorta. Cumulative concentration-response relationship for cirazoline in the aorta (**C**, n=9-10) and carbachol in the bladder (**D**, n=7-10) and bronchioles (**E**, n=6) from WT and miR-143/145 KO mice. **F, G** and **H** show summarized data for 60 mM KCl-induced contraction in WT and miR-143/145 KO mice. Panels **I, J** and **K** show contraction induced by the phosphatase inhibitor Calyculin A (1µM) in calcium free conditions in the aorta (**I**, n=6) bladder (**J**, n=6) and trachea (**K**, n=6-9) from WT and miR-143/145 KO mice. *p<0.05, **p<0.01 and ***p<0.001.

Figure 2. Opposing effects of miR-143/145 deletion on differentiation marker expression and smooth muscle volume in aorta and bladder
Transcript levels for contractile differentiation markers and transcription factors were examined in the aorta (**A**, n=6) and in the bladder (**B**, n=6) from WT and miR-143/145 KO mice. Primers for genes encoding myosin heavy chain (*Myh11*), desmin (*Des*), the L-type calcium channel pore forming subunit (*Cacna1c*), serum response factor (*Srf*), myocardin (*Myocd*) and Krüppel-like factor 4 and 5 (*Klf4*, *Klf5*) were used. 18S is used as housekeeping gene and aortic targets are normalized to WT aorta while bladder targets are normalized to WT bladder. **C** shows hematoxylin & eosin staining in the aorta and in the bladder from WT and miR-143/145 KO mice. **D** and **E** show compiled data on smooth muscle layer thickness in the aorta and bladder (n=4). *p<0.05, **p<0.01 and ***p<0.001.

Figure 3. Maintained basal actin polymerization in miR-143/145 KO smooth muscle
Rho-kinase (ROCK1) expression was analyzed by western blotting in aorta and bladder from WT and miR-143/145 KO mice (**A**, n=8). Western blot analysis was also performed for LIM-kinase (LIMK) phosphorylation ($LIMK1^{Thr508}$/$LIMK2^{Thr505}$) in the same organs (**B**, n=8). **C** shows the F/G actin ratio in aorta and bladder from WT and miR-143/145 KO mice (n=4). **D** and **F** show the protein expression of KLF-4 and KLF5, respectively. HSP90 was used as loading control and expression of all proteins are shown relative to the expression in bladder WT with the exception of the F/G actin ratio which is shown in absolute values. *p<0.05 and **p<0.01. §p<0.05 for bladder vs. aorta.

Figure 4. Deletion of miR-143/145 results in increased angiotensin converting enzyme (ACE) expression in aortic but not in bladder smooth muscle.
A and **B** show the mRNA and the protein expression of ACE in aorta and bladder in WT and miR-143/145 KO mice (n=6). Both mRNA and protein data are normalized to WT aorta. A representative western blot of ACE expression in aorta and bladder from the same gel demonstrates the difference in expression levels between these two tissues. Cumulative concentration-response curve of angiotensin II in aorta (**C**). Panel **D** shows the response to 10^{-7} M angiotensin II in aorta and bladder, respectively (n=6). *p<0.05, **p<0.01 and ***p<0.001. §p<0.05 for bladder vs. aorta.

Figure 5. Angiotensin receptor blockade rescues contractility in aorta with no effect in bladder smooth muscle. Panels **A** and **B** show concentrations response curves for cirazoline and carbachol in aortic rings and bladder strips after five days of organ culture with and without losartan (100µg/ml). Panels **C** and **D** show Calyculin A-induced force in aorta and bladder after culture in the absence and presence of losartan. *p<0.05, **p<0.01 and ***p<0.001.

Figure 6. Differential effects of miR-143/145 deletion on mRNA expression of RGS4 and RGS5 and angiotensin receptors in aorta versus bladder. Panels **A** and **B** show the mRNA expression of the

regulator of G signaling (Rgs) 4 and 5 in aorta and bladder from WT and miR-143/145 KO mice (n=6). Panels (**C**) and (**D**) show mRNA expression of AT_1 and AT_2 in aorta and bladder from WT and miR-143/145 KO mice (n=6). All targets were normalized to 18S and are shown relative to mRNA expression in WT aorta. *$p<0.05$ and **$p<0.01$.

Figure 1

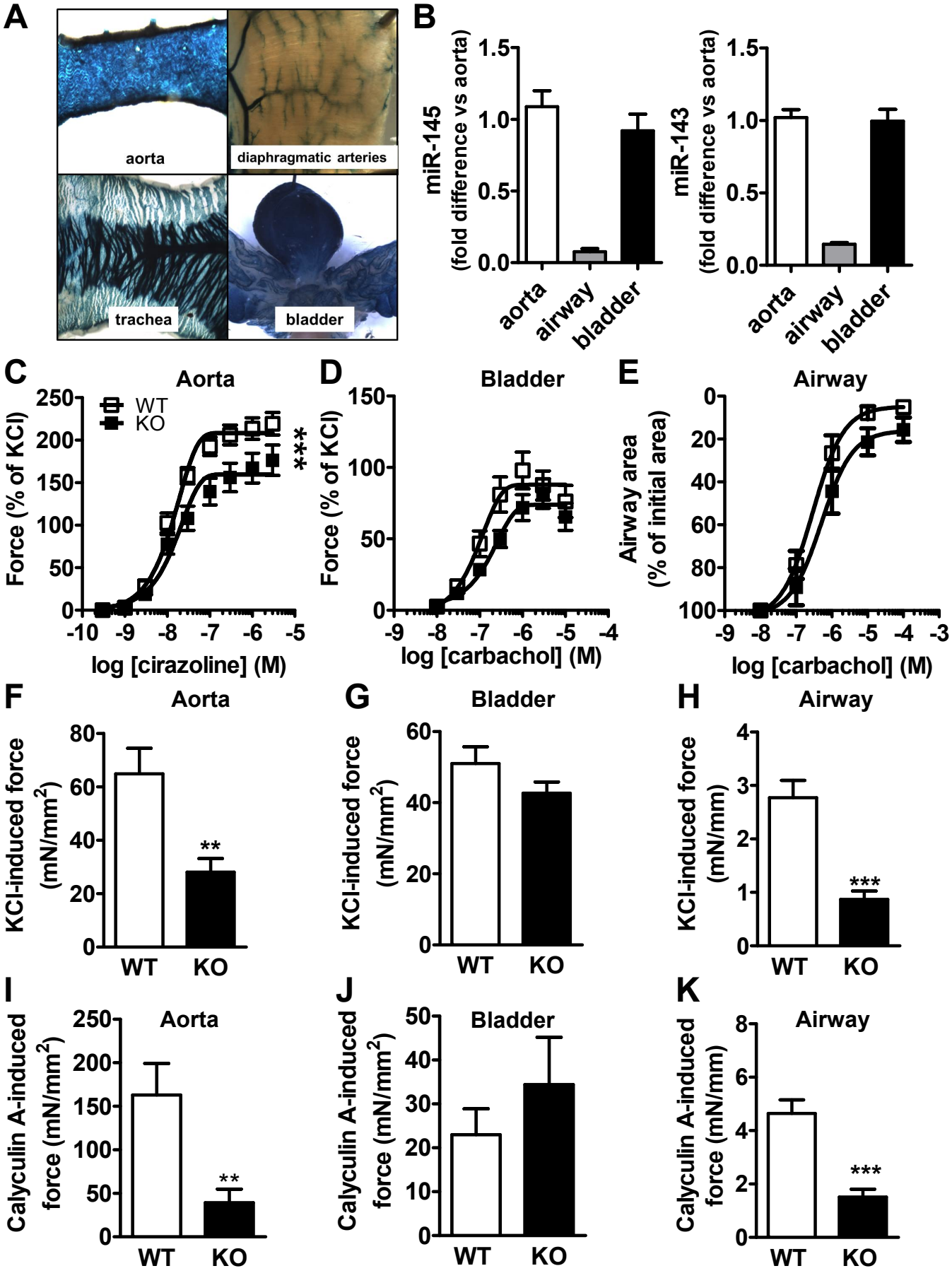
A
aorta
diaphragmatic arteries
trachea
bladder
B
miR-145
(fold difference vs aorta)
1.5
1.0
0.5
0.0
aorta
airway
bladder
miR-143
(fold difference vs aorta)
1.5
1.0
0.5
0.0
aorta
airway
bladder
C
Aorta
WT
KO
***
Force (% of KCl)
250
200
150
100
50
0
-10 -9 -8 -7 -6 -5
log [cirazoline] (M)
D
Bladder
Force (% of KCl)
150
100
50
0
-9 -8 -7 -6 -5 -4
log [carbachol] (M)
E
Airway
Airway area
(% of initial area)
0
20
40
60
80
100
-9 -8 -7 -6 -5 -4 -3
log [carbachol] (M)
F
Aorta
KCl-induced force
(mN/mm2)
80
60
40
20
0
**
WT
KO
G
Bladder
KCl-induced force
(mN/mm2)
60
40
20
0
WT
KO
H
Airway
KCl-induced force
(mN/mm)
4
3
2
1
0
***
WT
KO
I
Aorta
Calyculin A-induced
force (mN/mm2)
250
200
150
100
50
0
**
WT
KO
J
Bladder
Calyculin A-induced
force (mN/mm2)
50
40
30
20
10
0
WT
KO
K
Airway
Calyculin A-induced
force (mN/mm)
8
6
4
2
0
***
WT
KO

Figure 2

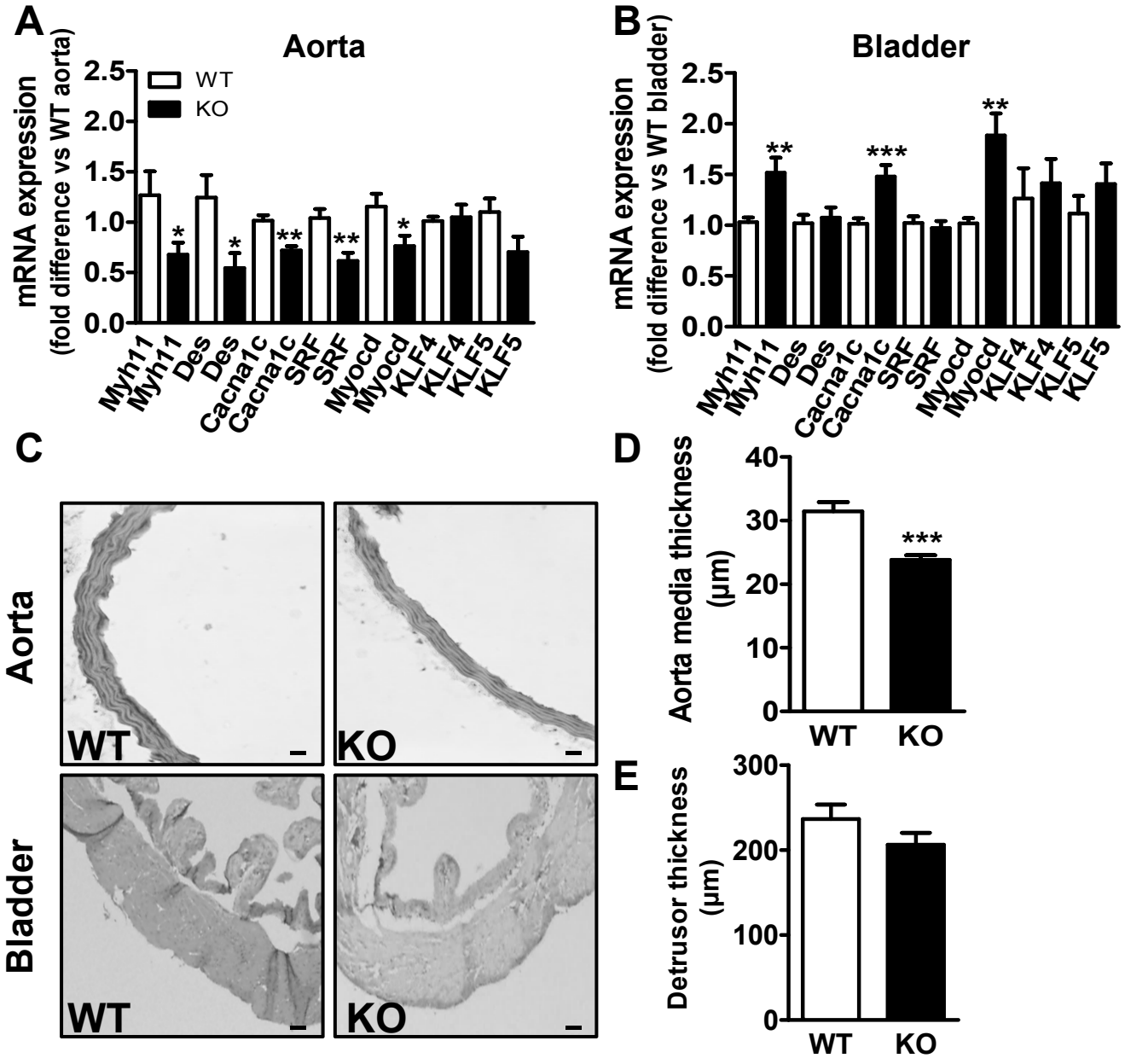
A
Aorta
mRNA expression
(fold difference vs WT aorta)
WT
KO
2.5
2.0
1.5
1.0
0.5
0.0
Myh11
Myh11
Des
Des
Cacna1c
Cacna1c
SRF
SRF
Myocd
Myocd
KLF4
KLF4
KLF5
KLF5
B
Bladder
mRNA expression
(fold difference vs WT bladder)
C
Aorta
Bladder
WT
KO
D
Aorta media thickness
(μm)
40
30
20
10
0
***
E
Detrusor thickness
(μm)
300
200
100
0

Figure 3

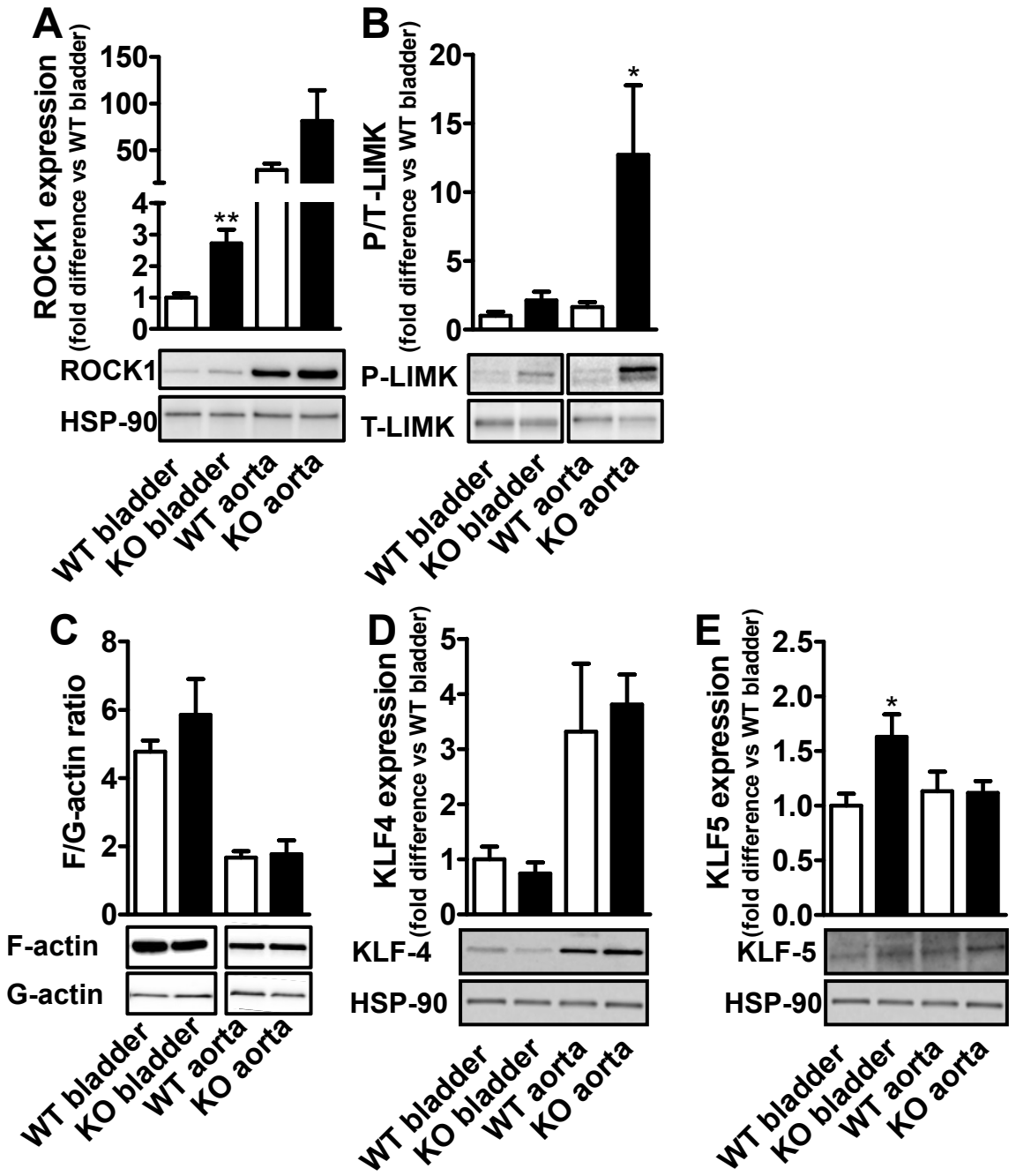
A
ROCK1 expression
(fold difference vs WT bladder)
150
100
50
4
3
2
1
0
**
ROCK1
HSP-90
WT bladder
KO bladder
WT aorta
KO aorta
B
P/T-LIMK
(fold difference vs WT bladder)
20
15
10
5
0
*
P-LIMK
T-LIMK
WT bladder
KO bladder
WT aorta
KO aorta
C
F/G-actin ratio
8
6
4
2
0
F-actin
G-actin
WT bladder
KO bladder
WT aorta
KO aorta
D
KLF4 expression
(fold difference vs WT bladder)
5
4
3
2
1
0
KLF-4
HSP-90
WT bladder
KO bladder
WT aorta
KO aorta
E
KLF5 expression
(fold difference vs WT bladder)
2.5
2.0
1.5
1.0
0.5
0.0
*
KLF-5
HSP-90
WT bladder
KO bladder
WT aorta
KO aorta

Figure 4

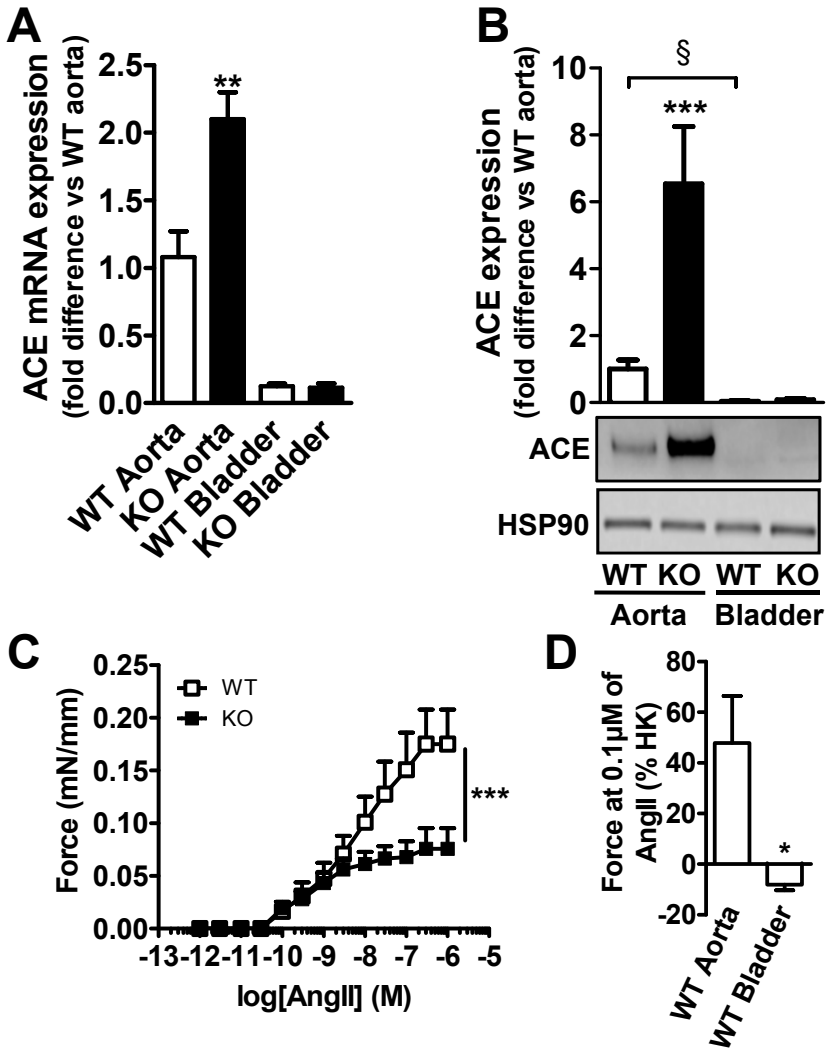
A
ACE mRNA expression
(fold difference vs WT aorta)
2.5
2.0
1.5
1.0
0.5
0.0
**
WT Aorta
KO Aorta
WT Bladder
KO Bladder
B
ACE expression
(fold difference vs WT aorta)
10
8
6
4
2
0
§
***
ACE
HSP90
WT KO WT KO
Aorta Bladder
C
Force (mN/mm)
0.25
0.20
0.15
0.10
0.05
0.00
WT
KO
***
-13 -12 -11 -10 -9 -8 -7 -6 -5
log[AngII] (M)
D
Force at 0.1µM of AngII (% HK)
80
60
40
20
0
-20
*
WT Aorta
WT Bladder

Figure 5

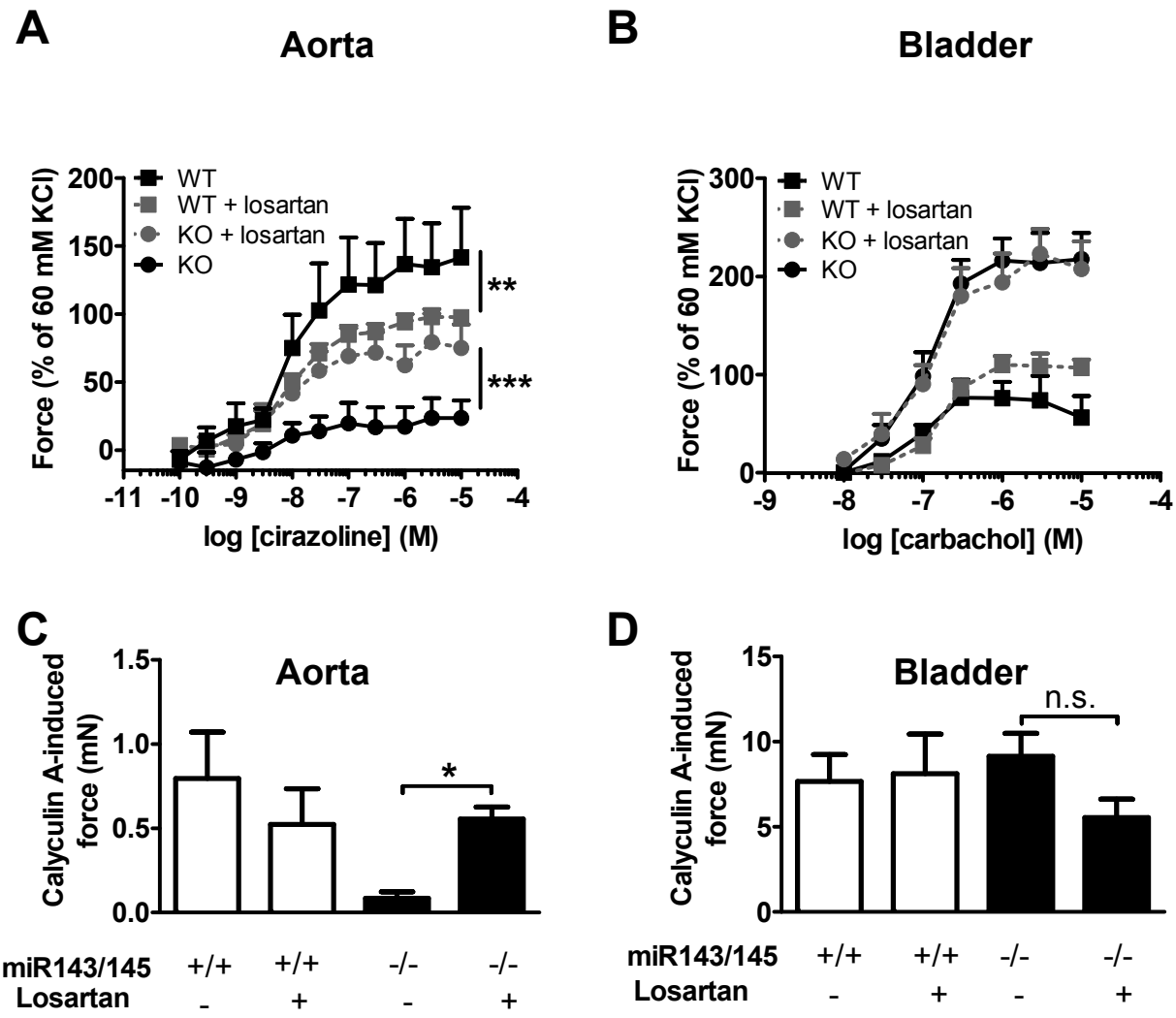
A
Aorta
WT
WT + losartan
KO + losartan
KO
Force (% of 60 mM KCl)
log [cirazoline] (M)
**
***
B
Bladder
log [carbachol] (M)
C
Aorta
Calyculin A-induced force (mN)
*
miR143/145
Losartan
+/+
+/+
-/-
-/-
-
+
-
+
D
Bladder
n.s.

Figure 6

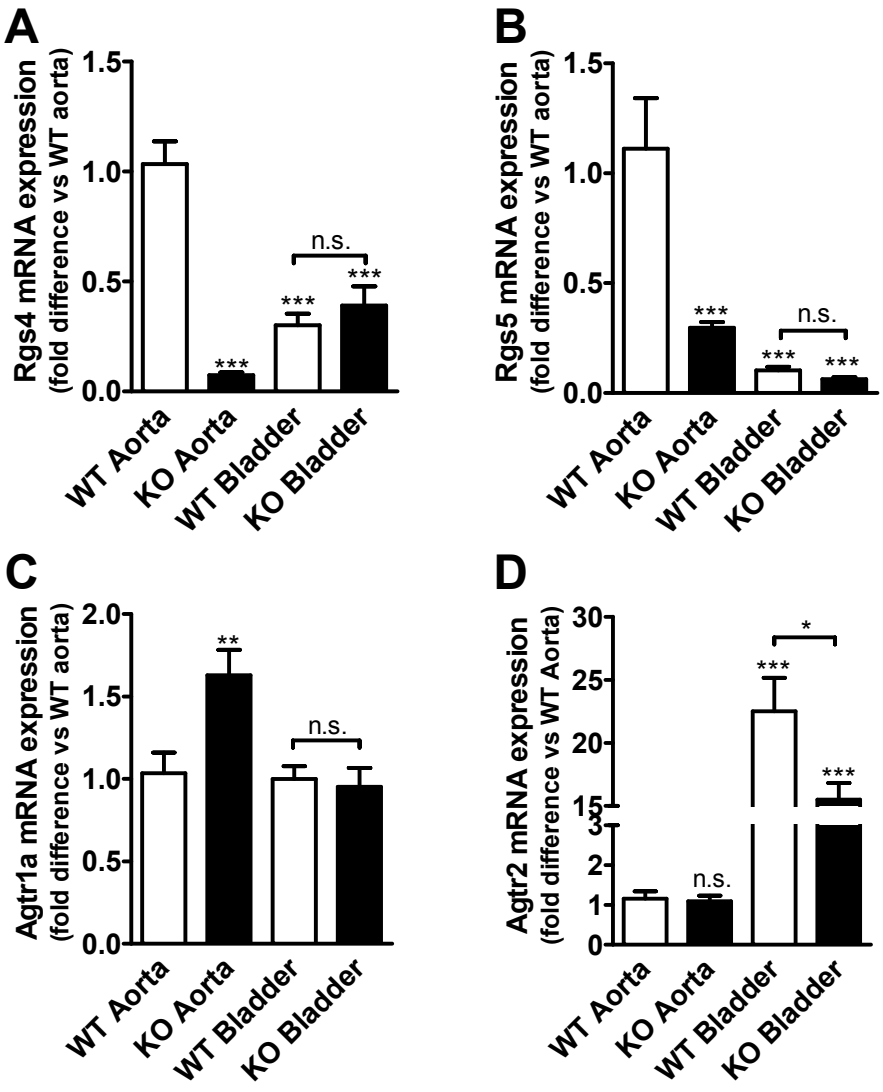
A
Rgs4 mRNA expression
(fold difference vs WT aorta)
1.5
1.0
0.5
0.0
***
***
n.s.
***
WT Aorta
KO Aorta
WT Bladder
KO Bladder
B
Rgs5 mRNA expression
(fold difference vs WT aorta)
1.5
1.0
0.5
0.0
***
n.s.
***
***
WT Aorta
KO Aorta
WT Bladder
KO Bladder
C
Agtr1a mRNA expression
(fold difference vs WT aorta)
2.0
1.5
1.0
0.5
0.0
**
n.s.
WT Aorta
KO Aorta
WT Bladder
KO Bladder
D
Agtr2 mRNA expression
(fold difference vs WT Aorta)
30
25
20
15
3
2
1
0
*
***
***
n.s.
WT Aorta
KO Aorta
WT Bladder
KO Bladder